Crystallographic Analysis of the Pseudomonas aeruginosa Strain K122-4 Monomeric Pilin Reveals a Conserved Receptor-Binding Architecture † , ‡

ARTICLE *in* BIOCHEMISTRY · OCTOBER 2004

Impact Factor: 3.02 · DOI: 10.1021/bi048957s · Source: PubMed

3 AUTHORS, INCLUDING:

Gerald Audette
York University
35 PUBLICATIONS **627** CITATIONS
SEE PROFILE

Randall T Irvin
University of Alberta
107 PUBLICATIONS **4,218** CITATIONS
SEE PROFILE

Crystallographic Analysis of the *Pseudomonas aeruginosa* Strain K122-4 Monomeric Pilin Reveals a Conserved Receptor-Binding Architecture[†,‡]

Gerald F. Audette, Randall T. Irvin, and Bart Hazes*

Department of Medical Microbiology and Immunology, University of Alberta, Edmonton, Alberta, Canada, T6G 2H7

Received May 21, 2004; Revised Manuscript Received July 2, 2004

ABSTRACT: Adherence of pathogens to host cells is critical for the initiation of infection and is thus an attractive target for anti-infective therapeutics and vaccines. In the opportunistic human pathogen *Pseudomonas aeruginosa*, host-cell adherence is achieved predominantly by type IV pili. Analysis of several clinical strains of *P. aeruginosa* reveals poor sequence conservation between pilin genes, including the residues in the receptor-binding site. Interestingly, the receptor-binding sites appear to retain a conserved surface epitope because all *Pseudomonas* type IV pili recognize the same receptor on the host cell and cross-reactive antibodies specific for the receptor-binding site exist. Here, we present the crystallographic analysis of two crystal forms of truncated pilin from *P. aeruginosa* strain K122-4 (ΔK122-4) at 1.54 and 1.8 Å resolution, respectively. The ΔK122-4 structure is compared to other crystallographically determined type IV pilin structures and an NMR structure of ΔK122-4 pilin. A comparison with the structure of the highly divergent *P. aeruginosa* strain K (ΔPAK) pilin indicates that the receptor-binding loop in both pilins forms a shallow depression with a surface that is formed by main-chain atoms. Conservation of this putative binding site is independent of the sequence as long as the main-chain conformation is conserved and could therefore explain the shared receptor specificity and antibody cross reactivity of highly divergent *Pseudomonas* type IV pilins.

The opportunistic pathogen *Pseudomonas aeruginosa* is a significant cause of morbidity and mortality in clinical settings. Acute *P. aeruginosa* infections observed in ventilator-associated pneumonia (*1*−*3*) and burn wounds (*4*−*6*) have high mortality rates. Furthermore, in individuals with a compromised or suppressed immune system, such as patients with cancer (*7*), cystic fibrosis (*8*, *9*) and HIV (*10*), *P. aeruginosa* can establish persistent infections that are frequently fatal through immune pathology, rather than the direct actions of the pathogen. Finally, the high innate and acquired antibiotic resistance of *P. aeruginosa* isolates complicate treatment (*11*, *12*). Therefore, the development of anti-infective agents against targets that bypass known resistance mechanisms is of considerable interest.

P. aeruginosa infection begins with the adherence of the pathogen to the epithelium, which is primarily achieved through the type IV pili. Consequently, type IV pili are an important virulence factor of *P. aeruginosa* (*13*) and other Gram-negative pathogens (*14*, *15*). Indeed, engineered strains of *P. aeruginosa* that lack functional pili exhibit reduced virulence (*16*, *17*). Also, a humoral response toward *P. aeruginosa* pili is protective (*18*−*20*). Type IV pili are fiber-like structures that are assembled from ∼15 kDa pilin monomers (*21*, *22*). Extensive studies on *P. aeruginosa* pilins have shown that each monomer contains a functional receptor-binding site within a disulfide-bound loop region (D-region; *16*, *23*−*29*). However, Lee and colleagues (*27*) demonstrated that receptor binding occurs only at the tip of the pilus, suggesting that the binding site is blocked during assembly except for the monomers exposed at the tip. In addition to cellular adhesion, the type IV pilus is involved in other processes such as twitching motility (*30*, *31*), biofilm formation (*32*−*34*), induction of host-cell signals (*35*−*37*), DNA uptake during natural transformation (*38*), and bacteriophage infection (*39*).

While pilins from different *P. aeruginosa* strains exhibit high sequence variability (*40*, *41*), it has been shown that they share specificity of the glycosphingolipids asialo-GM_1 and asialo-GM_2 that are present on the epithelial cells of the mucosal layer (*27*, *42*). In particular, Sheth et al. (*43*) demonstrated that the minimal receptor recognized by the pilin is the disaccharide β-D-GalNAc(1−4)β-D-Gal, a substructure of both asialo-GM_1 and asialo-GM_2. Furthermore, immunization with a peptide corresponding to the D-region of the pilin yields cross-reactive antibodies (*18*). Antibody cross reactivity and shared receptor specificity suggest that the receptor-binding domains of all *P. aeruginosa* strains

[†] This work was supported by operating grants from the Canadian Institutes for Health Research (MOP-38004 to R.T.I. and MOP-42448 to B.H.). X-ray diffraction data were collected at beamline 8.3.1 of the Advanced Light Source (ALS) at Lawrence Berkeley Lab, under an agreement with the Alberta Synchrotron Institute (ASI). The ALS is operated by the Department of Energy and supported by the National Institute of Health. Beamline 8.3.1 was funded by the National Science Foundation, the University of California, and Henry Wheeler. The ASI synchrotron access program is supported by grants from the Alberta Science and Research Authority (ASRA) and the Alberta Heritage Foundation for Medical Research (AHFMR). B.H. is an AHFMR scholar.

[‡] Coordinates and structure factor amplitudes for ΔK122-4 pilin have been deposited in the RCSB Protein Data Bank with accession codes 1QVE and 1RG0 for the triclinic and monoclinic crystal forms, respectively.

* To whom correspondence should be addressed. Phone: 780-492-0042. Fax: 780-492-7521. E-mail: bart.hazes@ualberta.ca.

10.1021/bi048957s CCC: $27.50
Published on Web 08/18/2004

have retained a conserved surface epitope despite the poor sequence conservation.

Crystal structures of the full-length *Neisseria gonorrhoeae* strain MS11[1] (*44*) and *P. aeruginosa* strain K (PAK; *45*) pilins have been reported, but structure determination of full-length pilins is complicated by poor solubility. Full-length pilins contain a long N-terminal α-helix (α1). The first 28 residues (α1-N) are exposed and highly hydrophobic, whereas residues 29−54 (α1-C) pack onto the globular head domain of the pilin. Truncation of α1-N results in a soluble pilin monomer that retains the receptor-binding characteristics of the intact pilin (*41*; Irvin, R. T., unpublished data). To date, crystal structures of the truncated PAK pilin (ΔPAK; *40*) and *Vibrio cholerae* toxin-coregulated pilin (*45*) have been reported, as well as an NMR structure of truncated pilin from *P. aeruginosa* strain K122-4 (ΔK122-4^{NMR}; *41*). However, the region of greatest interest, the C-terminal receptor-binding domain, could not be unambiguously assigned in the NMR study because of spectral overlap (*41*).

In this paper, we present the structures of two crystal forms of the ΔK122-4 pilin refined to 1.54 and 1.8 Å resolution, respectively. We compare the ΔK122-4 structure with other crystallographically determined type IV pilin structures and with the structure of ΔK122-4 previously determined using NMR spectroscopy (ΔK122-4^{NMR}; *41*). This presents the first opportunity to compare the receptor-binding sites of two highly divergent pilins that share receptor specificity (the *V. cholerae* pilin has no equivalent binding site, and to our knowledge, receptor specificity for MS11 pilin has not been reported). The comparison supports our earlier hypothesis that the type IV pilins of *P. aeruginosa* have a binding site consisting predominantly of main-chain atoms. Conservation of function is therefore independent of sequence as long as the main-chain conformation is retained.

EXPERIMENTAL PROCEDURES

Crystallization and Data Collection. Purification, crystallization, and X-ray diffraction data collection for the triclinic form of ΔK122-4 pilin has been reported previously (*46*). Briefly, ΔK122-4 [*pilA*(Δ1−28); *41*] was expressed periplasmically in *Escherichia coli* as a maltose-binding-protein (MBP) fusion protein and purified using an amylose column (*46*). The purified MBP−K122-4 fusion protein was trypsinized to release ΔK122-4 pilin from MBP. The monomeric ΔK122-4 pilin contains four N-terminal residues (ISEF) from the expression construct followed by residues 29−150 of K122-4 pilin. Monomeric ΔK122-4 was then purified by cation-exchange chromatography and crystallized as described (*46*). The monoclinic crystal form of ΔK122-4 pilin crystallized under conditions similar to that of the triclinic form but in the presence of the receptor analogue β-D-GalNAc(1−4)β-D-Gal-OMe. Crystals were grown from 2-μL drops containing equal volumes of protein−carbohydrate solution (20 mg mL^{-1} ΔK122-4 and 15.7 mM β-D-GalNAc(1−4)β-D-Gal-OMe in 10 mM Tris at pH 7.4 and 100 mM sodium chloride) and reservoir solution (38% w/v PEG 4000, 100 mM sodium cacodylate at pH 5.8, and 100 mM monobasic potassium phosphate). Diffraction data were collected on beamline 8.3.1 at the Advanced Light Source and were processed using MOSFLM (*47*) and SCALA from the CCP4 suite (*48*). A summary of the diffraction and refinement statistics is shown in Table 1.

Table 1: Summary of Diffraction and Refinement Statistics

diffraction statistics		
space group	$P1$	$P2_1$
cell a, b, c (Å)	40.19, 38.93, 37.22	37.30, 80.72, 39.13
cell α, β, γ (deg)	66.38, 111.11, 93.74	90.0, 113.37, 90.0
resolution (Å)	37−1.54	40.5−1.80
observed reflections	62 889	47 085
unique reflections	26 457	16 181
completeness (%)[a]	93.1/88.5	82.8/76.4
average $I/\sigma I$)[a]	16.5/6.6	6.4/2.0
R_{sym} (%)[a,b]	5.9/9.6	19.2/39.1
refinement statistics		
resolution range (Å)	35.4−1.54	40.5−1.80
number of reflections	25 365	16 158
total protein non-H atoms	1789	1798
solvent molecules	289	89
R_{work} (%)[c]	13.8	23.6
R_{free} (%)[d]	17.6	25.4

[a] Overall/highest resolution shell. [b] R_{sym} is the unweighted R value between symmetry mates. [c] $R_{work} = \sum_{hkl}||F_{obs}(hkl)| - |F_{calc}(hkl)||/\sum_{hkl}|F_{obs}(hkl)|$. [d] R_{free} is the cross validation R factor using 5% of reflections.

Structure Solution and Refinement. The structures of both crystal forms of the ΔK122-4 pilin were solved using molecular replacement (MR) and employed the AMoRe software package (*49*) of the CCP4 suite (*48*). For the triclinic crystal form, the molecular replacement search model was the globular domain of the MS11 pilin (PDB ID 1AY2; *44*), from which nonconserved regions were removed. Analysis of the self-rotation function revealed a single peak 13σ above the background ($\kappa = 180°$), indicating that there is a ΔK122-4 dimer in the unit cell (*46*). To determine the initial positions of the two ΔK122-4 molecules, the top rotation peak was interpreted as the first ΔK122-4 molecule and then fixed. With the top peak fixed, the subsequent 10 rotation peaks were employed in the translation search to determine the position of the second ΔK122-4 pilin molecule relative to the first. After the initial coordinates for both molecules were obtained, rigid-body refinement in AMoRe resulted in a correlation coefficient and R value of 0.490 and 0.468, respectively.

The MR solution was used as input for ARP/wARP (*50*, *51*) to fill in the nonconserved regions that were removed from the MS11 search model. After removal of the dummy atoms generated by ARP/wARP, examination of an initial σ_A-weighted (*52*) $2F_o - F_c$ electron density map in Xfit (*53*) allowed for the building of all residues with the exception of Ile 25 and Ser 26 of chain A and Thr 149 and Pro 150 of chain B. These residues, with the exception of Pro 150B, were located during subsequent rounds of refinement. Residue 36 has been reported as Arg in the sequence database (gi|77636; *54*). However, our sequencing demonstrated that residue 36 was in fact an Ala. Alanine is also more consistent with the preference for a small residue at this position in other pilin sequences (*40*), and an Arg would be incompatible because of steric constraints. Accordingly, we feel that an Ala is the correct residue at this position. The model was

[1] Abbreviations: ΔK122-4, the truncated *Pseudomonas aeruginosa* strain K122-4 pilin; ΔK122-4^{NMR}, the truncated K122-4 pilin solved using NMR; MS11, the *Neisseria gonorrhoeae* strain MS11 pilin; PAK, the *P. aeruginosa* strain K pilin; ΔPAK, the truncated PAK pilin; rmsd, root-mean-square deviation; NCS, noncrystallographic symmetry; NMR, nuclear magnetic resonance spectroscopy.

refined using REFMAC (*55*), and TLS parameters (*56*) were refined prior to refining atomic positions and isotropic *B* factors. All data were used during the refinement, with 1336 reflections being set aside for R_{free} calculation (*57*) and σ_A estimation. Engh and Huber (*58*) stereochemical restraints and loose noncrystallographic symmetry (NCS) restraints were employed throughout the refinement. Rounds of refinement were followed by model building in Xfit using σ_A-weighted density maps. Solvent atoms were located using ARP/wARP and confirmed with visual inspection. Several residues were modeled with alternative side-chain conformations based on the shape of the electron density; the occupancies of these alternative conformations were refined using SHELXL (*59*). Restrained individual anisotropic *B* values were refined in the final cycle. The validity of the anisotropic *B* value refinement at this resolution was supported by the R_{free} statistic, which dropped from 18.1 to 17.8%. The refinement statistics are summarized in Table 1.

The structure of the monoclinic form of the ΔK122-4 pilin was solved using the refined structure of triclinic ΔK122-4 pilin (protein only) as the MR search model. The correlation coefficient and *R* value following molecular replacement were 0.721 and 0.312, respectively. The model was refined using a similar strategy as that for the triclinic crystal, with 661 reflections being set aside for R_{free} calculation and σ_A estimation. Occupancies for residues with alternative conformations were refined using SHELXL. A summary of refinement statistics is shown in Table 1.

RESULTS AND DISCUSSION

Quality of the Final Models. The structure of the triclinic crystal form of ΔK122-4 pilin was refined to 1.54 Å resolution, with a NCS-related pilin dimer (chains A and B) in the P1 unit cell. R_{work} and R_{free} were refined to 13.8 and 17.6%, respectively. In the final model, all residues except the C-terminal residue (Pro 150) of chain B were observed and 289 water molecules could be modeled in the electron density. Five residues were modeled with dual side-chain conformations. These residues are Ser 34, Thr 45, Ser 48, Ser 56, and Cys 142 and are all located in chain A. Only Lys 140 of chain A did not show electron density for its side chain, and atoms past C^β were therefore not included in the final model. The average *B* factors (main chain/side chain) are 6.6 Å^2/8.3 Å^2 and 6.6 Å^2/8.5 Å^2 for chain A and B, respectively, and 24.4 Å^2 for the solvent molecules. Analysis of the stereochemical quality of the final model using PROCHECK (*60*) indicated that all residues are in the core or allowed regions of the Ramachandran plot (*61*), and no strained stereochemical conformations were observed.

The monoclinic crystal form of ΔK122-4 pilin was obtained during cocrystallization trials of the pilin with its carbohydrate receptor analogue β-D-GalNAc(1−4)β-D-Gal-OMe. The structure also contains an NCS-related dimer within the asymmetric unit and was refined to 1.8 Å resolution. The final R_{work} and R_{free} values are 23.6 and 25.4%, respectively. The final model consists of all 126 residues in each pilin monomer and 89 solvent molecules. Unfortunately, no electron density corresponding to bound carbohydrate was observed in a difference electron density map prior to the addition of solvent molecules or any map thereafter. The tight packing of the pilin in the crystal, weak affinity for the receptor, and presence of the C-terminal tail of the pilin monomer (see below) likely prevented complex formation. Average *B* factors (main chain/side chain) are 10.6 Å^2/13.6 Å^2, 12.1 Å^2/16.5 Å^2, and 30.7 Å^2 for chains A and B and solvent molecules, respectively. Four residues were observed to have dual conformations: Ser 56A, Cys 57A, Cys 142A, and Ser 56B. The alternate conformations of the cysteines in both crystal forms are believed to result from radiation damage as was earlier observed for ΔPAK (Hazes, B., unpublished results). Analysis of the stereochemical quality of the final model using PROCHECK identified that 90.9% of all residues are within the core regions of the Ramachandran plot, 8.6% are within allowed regions, and a single residue, Ala 65 of chain B, is within a generously allowed region. The only significant deviation from stereochemical ideality was the C−N−C$^\alpha$ angle between Thr 61 and Ala 62 of both chains. This region has weak electron density and may exhibit some disorder that could not be modeled at the present resolution. Diffraction and refinement statistics for both crystal forms are summarized in Table 1.

The four ΔK122-4 monomers in our crystal forms show minimal differences, with root-mean-square deviations (rmsd's) between all C$^\alpha$ positions ranging from 0.22 to 0.67 Å. Unless otherwise specified, all analyses presented below are based on chain A of the high-resolution triclinic crystal form, which is most clearly defined by its electron density. Both crystal forms of ΔK122-4 contain equivalent NCS-related dimers in the asymmetric unit. Pilin dimers have also been observed in the crystal structures of MS11 (*44*) and PAK (*45*); however, these dimers are distinct from each other and from our ΔK122-4 dimers. Also, there is no evidence for a functional role for type IV pilin dimers, and dimerization of ΔK122-4 was not observed in NMR or equilibrium centrifugation studies (*41*). Therefore, the observed ΔK122-4 dimers appear to have no biological relevance and likely arise because of crystallization conditions.

Common Architecture of the Type IVa Pilins. The structures of four type IV pilins have been described in the literature. Three have been examined crystallographically: the *N. gonorrhoeae* strain MS11 pilin (*44*), the truncated toxin-coregulated pilin from *V. cholerae* (*45*) and the *P. aeruginosa* strain K pilin, both as truncated (ΔPAK; *40*) and full-length (PAK; *45*) pilins. The fourth type IV pilin, the ΔK122-4 pilin, has been examined via NMR methods (ΔK122-4^{NMR}; *41*). The toxin-coregulated pilin, classified as a type IVb pilin, differs significantly in size, leader sequence, monomer sequence, and structure from the *Pseudomonas* and *Neisseria* type IVa pilins (*45*, *62*). Accordingly, it is not included in the present analysis.

The ΔK122-4 crystal structure exhibits the characteristic type IVa pilin fold, with the N-terminal α-helix (α1-C) packed onto a four-stranded antiparallel β-sheet (Figure 1a). The relative positions of the core secondary structure elements are well-conserved among the crystal structures (Figure 1b), and structural superimpositioning gives C$^\alpha$ rmsd values of 1.0−1.4 Å (Table 2). Interestingly, ΔK122-4 most closely resembles MS11 rather than ΔPAK even though MS11 pilin is of Neisserial rather than Pseudomonal origin. A closer phylogenetic relationship between K122-4 and MS11 pilin is also evident at the amino acid sequence level with 46.1% sequence identity between K122-4 and MS11

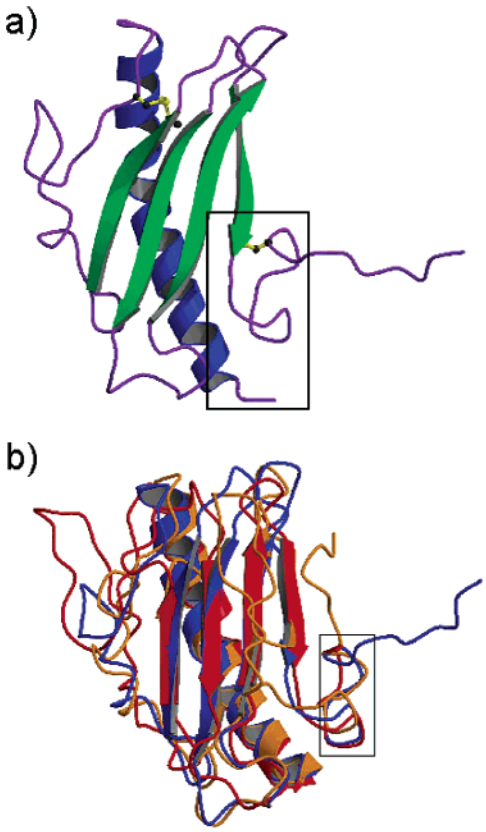

FIGURE 1: Structure of the ΔK122-4 pilin and the common tertiary structure of the type IVa pilins. (a) ΔK122-4 pilin monomer. The N-terminal α-helix (α1-C) is in blue; the *β*-sheet is in green; and the coil regions are in purple. The two disulfide bridges observed in ΔK122-4, between Cys 57 and 93 and between Cys 129 and 142, are shown in yellow. (b) Superimposition of the ΔK122-4 (blue), ΔPAK (red; *40*), and MS11 (orange; *44*) pilins, highlighting the conserved structural architecture of the type IVa pilins. In both panels, the conserved receptor-binding domain of the *Pseudomonas* pilins is boxed. All figures were produced using MOLSCRIPT (*70*) and Raster3D (*71*).

Table 2: Structural and Sequence Similarity between the Type IVa Pilins[a]

	ΔK122-4	ΔK122-4^{NMR}	MS11	ΔPAK
ΔK122-4		1.2/37	1.0/88	1.2/59
ΔK122-4^{NMR}	100%		4.9/88	1.8/30
MS11	42%	42%		1.4/60
ΔPAK	29%	40%	27%	

[a] Superposition of the C^{α} atoms of the various pilins performed using SUPPOS (Dijkstra, B. W., unpublished results). Above the diagonal: rmsd (Å)/number of residues superimposed. Below the diagonal: percentage of sequence identity between structurally superimposed residues.

versus 38.8% sequence identity between K122-4 and PAK (these values are 36.3 and 26.1%, respectively, for the globular domain sequence starting at residue 29; Table 2). These observations indicate that the large sequence variations seen between pilin genes in different *P. aeruginosa* isolates originate at least in part from horizontal gene transfer.

Surprisingly, a global rmsd could not be calculated between the ΔK122-4 structures determined by crystallography and NMR because of differential packing of the helix and sheet in the two structures (Figure 2). If we first superimpose the average ΔK122-4^{NMR} structure onto ΔK122-4 based on their *β*-sheets, 37 residues superimpose with an rmsd of 1.2 Å (Table 2). An additional 44.5° rotation and 3.9 Å translation are required to subsequently superimpose the α helices. Analysis of the 10 individual ΔK122-4^{NMR} models in the NMR ensemble gave basically the same results. It has been speculated that the disulfide bond between Cys 57 and Cys 93 may have caused the different helix−sheet packing (*41*), but this disulfide bond in both X-ray and NMR structures is actually well-conserved (Figure 2). Because neither cysteine is part of the α-helix, it is not obvious from the structure how this disulfide would change the helix packing.

In ΔK122-4^{NMR}, the α-helix is shifted down by one turn and is deflected away from the *β*-sheet, especially at the N-terminal end of the α-helix (Figure 2). As a consequence, the packing of the hydrophobic core is less tight in ΔK122-4^{NMR} and a conserved hydrogen bond between the O^{ϵ} of Gln 32 and the amide nitrogen of Ala 105 is missing. Because all crystal structures, with several determined at high resolution, reveal a consistent helix−sheet packing, we believe that they represent an accurate and relevant conformation of the pilin. The deviation observed in ΔK122-4^{NMR} could be due to one or more incorrect NOE assignments. However, a comparison of the NMR restraint data with both the NMR and X-ray structures suggests that this is not the case. There are also data that indicate structural flexibility of the pilin monomer. Molecular models of type IV pili generated using the crystal structures of ΔPAK and MS11 only explain X-ray fiber diffraction patterns when the globular domain is omitted from calculations of simulated diffraction patterns (*63*). This suggests a disorder of the globular domain relative to the helical backbone. Furthermore, *Neisseria* pilins can be proteolytically cleaved in vivo after residue 39 to release a soluble pilin monomer (*64*). Residue 39 is in the middle of the α-helix (α1), and this peptide bond would not be accessible for proteolytic cleavage when α1 is tightly packed against the *β*-sheet as seen in the crystal structures. It is therefore possible that under physiological conditions the *β*-sheet is able to move relative to the α-helix, whereas the high concentrations of precipitants used for crystallization may have stabilized the tighter packing. Further research will be required to directly address this question.

The loop connecting α1-C to the *β*-sheet (the α*β*-loop) is highly variable in sequence and structure. In PAK, a small *β*-sheet follows α1-C, whereas in MS11, the equivalent space is occupied by a single helical turn that is glycosylated at Ser 63. In models for the type IV pilus fiber (*40*, *44*, *62*), these structural features block the receptor-binding site of a pilin monomer in the preceding turn of the pilus fiber. It has been proposed that this may explain why receptor binding only occurs at the tip of the pilus (*40*). ΔK122-4 pilin does not have the small *β*-sheet of PAK pilin, and while Thr 64 of ΔK122-4 is within 5 Å of the glycosylated Ser 63 of MS11, *P. aeruginosa* strain K122-4 pilin is not glycosylated (*65*; Irvin, R. T., unpublished results). Therefore, the loop of ΔK122-4 does not appear to provide a bulky group that can block receptor-binding sites along the flanks of the pilus. Two alternative, though speculative, mechanisms for occluding the receptor-binding domain in the pilus fiber can be envisioned. The first involves the C-terminal extension. While other *P. aeruginosa* pilins have only two to three residues following the C-terminal cysteine, K122-4 has eight

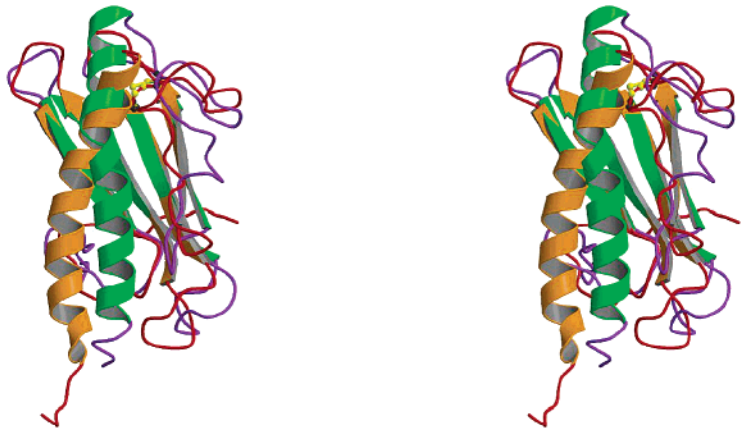

FIGURE 2: Stereoview of the superimposed models of ΔK122-4 as determined by NMR (red and orange) and X-ray crystallography (green and purple). Both structures were superimposed based upon their β-sheets, showing the deflection of α1-C in the NMR structure. The disulfide bond between Cys 57 and Cys 93, shown in yellow, superimposes well and is therefore unlikely to have caused the helix deflection as previously proposed (*41*).

residues (*40*). NMR observations indicate that the C-terminal extension is highly disordered in solution (*41*), and no intramolecular interactions are seen in our crystal structures. It is conceivable that the C-terminal extension is disordered when exposed at the pilus tip, providing access to the binding sites, whereas it may adopt a conformation that blocks the binding sites when buried upon pilus assembly. The second possible mechanism is that the unstructured αβ-loop could adopt an alternate conformation during pilus assembly that would occlude the receptor-binding domain.

Receptor-Binding Domain. Multiple studies using a variety of techniques have localized the receptor-binding domain of the *P. aeruginosa* type IV pilins to a 14−19-residue disulfide-bound loop at the C terminus of the protein (the D-region). Antibodies targeting the D-region but not other regions of the pilin are able to inhibit *Pseudomonas* adherence (*24*, *26*). Mutations in the D-region do not affect pilus biogenesis, but both cell binding and virulence were significantly reduced (*16*). Further, peptides that represent the disulfide-bound D-region competitively inhibit pilus binding to buccal epithelial cells (*25*), and direct interaction between such a peptide and a receptor analogue has been demonstrated by NMR (*29*). It has also been shown that the type-IV pilins bind to the same receptor (*27*, *42*) and display a conserved antigenic epitope (*29*). The latter observation has led to the development of a strain-independent peptide-based vaccine candidate, using a consensus sequence derived from several D-region sequences (*18*−*20*).

The structure of the D-region was first studied by NMR using synthetic peptides with sequences derived from several highly divergent *P. aeruginosa* strains (*28*, *65*, *66*). These studies showed that all peptides contained two β turns and a type I turn (residues 134−137) followed by a type II turn (residues 139−142). NMR studies of a D-region peptide in complex with a receptor analogue or a cross-reactive antibody indicated little structural rearrangement upon complex formation (*29*). Apparently, these peptides have an "intrinsic propensity" to adopt a native-like conformation despite the high sequence divergence.

The ΔPAK crystal structure confirmed the presence of the two β turns in the D-region with the main difference being a somewhat different relative orientation of the β turns. Interestingly, the β turn geometry creates one face of the turn that exposes only main-chain atoms, and the relative orientation of the two β turns is such that a shallow solvent-exposed pocket is formed that is dominated by main-chain atoms (*40*; Figures 1 and 3). Several carbonyl oxygen and amide nitrogen atoms of the main chain point up into the pocket and could potentially act as hydrogen-bonding partners for hydroxyl groups of the carbohydrate ligand. This led to the hypothesis that the pocket formed by the two β turns forms a unique main-chain-atom-dominated receptor-binding site (*40*). Shared receptor specificity and antibody cross reactivity by highly divergent pilins could then result from conservation of the main-chain structure because of evolutionary constraints.

To better understand the conformational determinants of the D-region, we looked at conserved properties of the *P. aeruginosa* pilin sequences. There are seven strictly conserved residues in the globular domain of *Pseudomonas* pilins (*40*); in K122-4, these residues are Arg 30, Lys 44, Thr 98, Trp 127, Cys 129, Pro 139, and Cys 142. Within the D-region, only the two cysteines that form the disulfide and proline 139 that starts the second β turn are strictly conserved. Disulfide bonds and proline residues restrict the conformational flexibility of peptides and therefore likely play a structural role in defining the conformation of the D-region. Studies have indeed shown the importance of the disulfide bond for structure and function of synthetic receptor-binding loop peptides (*28*, *29*, *66*−*69*). In the pilin structures, the side chains of the cysteine and proline residues are buried between the loop and the core of the protein. This also points to a structural rather than a functional role because the residues cannot directly interact with the receptor but instead define the loop−protein packing interface. Tyr 137 also contributes to this packing interface, and an aromatic amino acid is conserved at this position in the loop (*40*). Furthermore, in the ΔK122-4 structure, the strictly conserved Arg 30 stabilizes the D-region through hydrogen bonds between its N^{ϵ} and N^{H1} atoms and the carbonyl oxygen of Lys 136 (Figure 3a). The conserved Trp 127 and Lys 44 interact with each other, forming a hydrophobic stacking interaction between the α-helix and β-sheet. This interaction is important to stabilize the globular domain structure but should not directly influence the D-region structure. Finally, Thr 98 is exposed to the solvent and not close to the D-region. Its

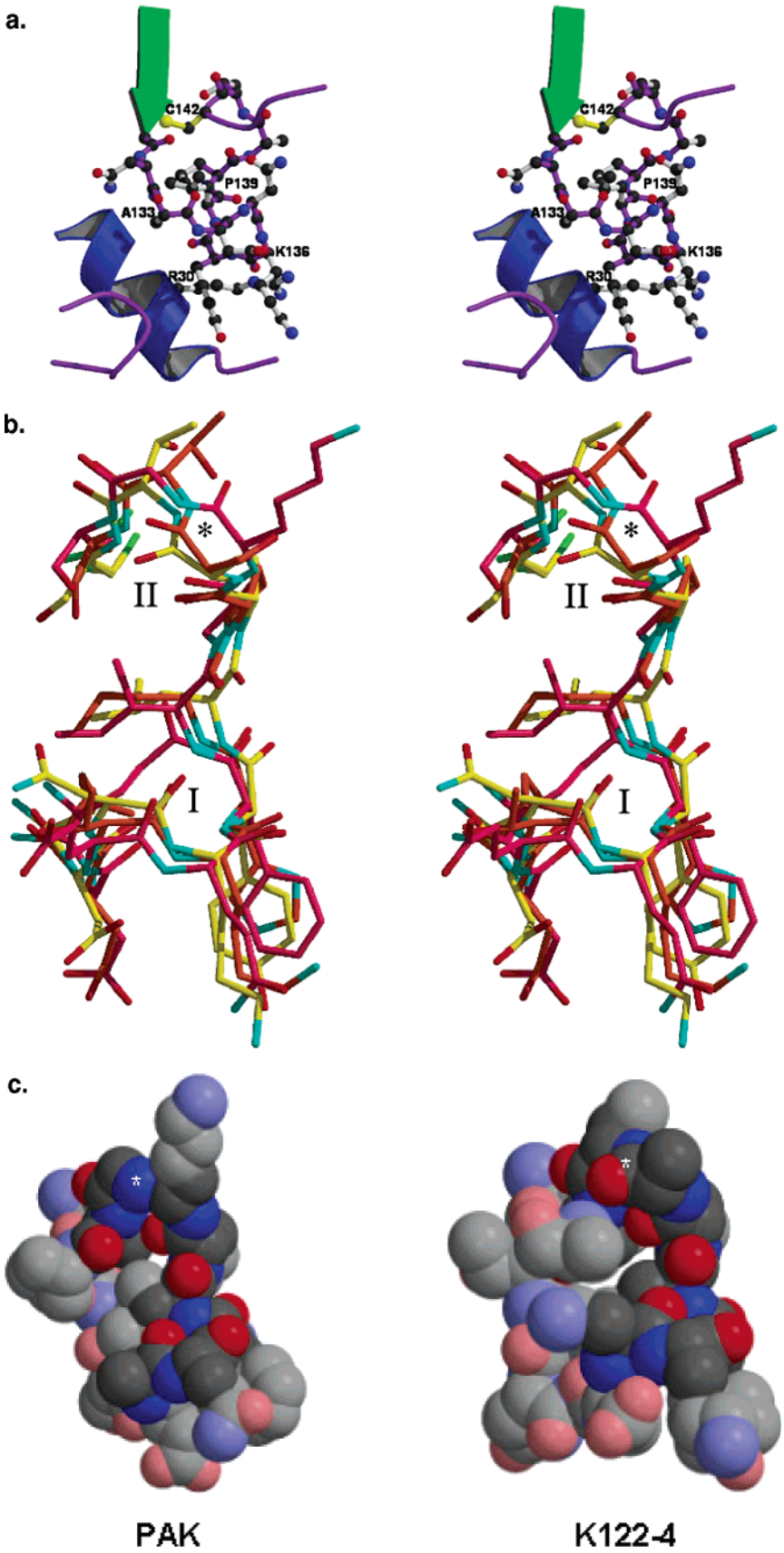

FIGURE 3: Receptor-binding domain of the type IVa pilins. (a) Stereoview of the ΔK122-4 receptor-binding domain (boxed in Figure 1a). All residues of the receptor-binding loop and the conserved Arg 30 are shown in a ball-and-stick representation. (b) Stereorepresentation of the superimposed receptor-binding loop of ΔK122-4, ΔPAK, and MS11 pilins (boxed in Figure 1b). Backbone atom colors are yellow, magenta, and orange, respectively. The two β turns are labeled I and II, and the peptide flip at residue 141 in ΔPAK is labeled with an asterisk. (c) CPK representation of the PAK and K122-4 D-regions showing the surface-exposed atoms. Main-chain atoms of the residues that form the two β turns are in darker colors, highlighting the conserved surface of the proposed receptor-binding site. The peptide flip has again been highlighted with an asterisk.

role in the structure or function of pilin, if any, is at this moment unclear.

The D-region of ΔK122-4 exhibits, as expected, a main-chain structure that is largely conserved when compared with that of ΔPAK (Figure 3). The main difference between ΔPAK and ΔK122-4 is a flip of the peptide plane between residues 140 and 141 in ΔK122-4. This changes the type II β turn into a type III β turn. In ΔPAK, residue 141 adopts a distorted left-handed helical conformation that is only allowed for glycine (present in PAK, PAO, and KB7 pilins) and, to a lesser extent, asparagine (present in P1 pilin; *40*). In contrast, the threonine present in K122-4 and the *Neisseria* pilins is not compatible with a left-handed helical conformation, resulting in the peptide flip. This is a very local structural change that may not affect receptor binding if the peptide plane carbonyl oxygen does not contact the receptor. It is also of interest to note that a water molecule in optimal hydrogen-bonding geometry with the main-chain nitrogen of Gly 141 in ΔPAK would have a position that coincides with the carbonyl oxygen of Lys 140 in ΔK122-4. Accordingly, an interaction by the carbonyl oxygen in ΔK122-4 could be replaced by a water-mediated interaction in ΔPAK. Finally, although Thr 141 prevents ΔK122-4 from adopting a ΔPAK-like β turn, it is possible that ΔPAK can adopt a type III β-turn conformation upon receptor binding. The structure of a pilin in complex with a carbohydrate analogue is required to delineate the receptor-binding determinants of the binding pocket and to fully evaluate the impact of the peptide flip on receptor binding.

The ΔPAK and ΔK122-4 receptor-binding pockets also show one difference with respect to amino acid side chains. Whereas the binding pocket is devoid of any side chains in the ΔPAK structure, the pocket is occupied by the side chain of Gln 143 in the ΔK122-4 structure (Figure 3b). However, Gln 143 is part of the C-terminal extension that was found to be highly flexible in the NMR structure (*41*). Indeed, in the NMR ensemble of structures, Gln 143 typically does not block the receptor-binding pocket. It is tempting to hypothesize that the NMR structure resembles a tip-exposed binding site, whereas the crystal structure reflects the situation for nontip-exposed monomers where protein−protein interactions cause the C terminus to block the binding pocket. However, because the crystal-packing interface will differ from the protein−protein interactions in the pilus fiber, this hypothesis remains to be confirmed.

We have solved the crystal structure of ΔK122-4 pilin to determine the features in the receptor-binding site that have been conserved between the ΔK122-4 and ΔPAK pilins. We found that the main-chain structure of the D-region was conserved between both pilins. This supports our earlier hypothesis that highly divergent *P. aeruginosa* type IV pilins share a receptor-binding site that is formed by main-chain atoms and that receptor specificity and antigenic characteristics are conserved by conservation of the main-chain structure. Interestingly, the D-region in *Neisseria* MS11 pilin is very similar to especially the ΔK122-4 pilin (Figure 3b) even though it has to accommodate a 17-residue insertion. This suggests that the D-region in *Neisseria* and *Pseudomonas* may share a common function. Such a function does not have to be limited to receptor binding because type IVa pili are associated with many other functions such as twitching motility, biofilm formation, and DNA binding (*31*, *33*, *62*). A potential role for the D-region in these additional pilus-associated functions is currently under investigation.

ACKNOWLEDGMENT

We thank A. M. Brigley and L. Price for technical assistance and J. P. Bacik, C. Giltner, and E. J. van Schaik for useful discussions.

REFERENCES

1. Todd, T. R. J., Franklin, A., Mankinen-Irvin, P., Gurman, G., and Irvin, R. T. (1989) Augmented bacterial adherence to tracheal epithelial cells is associated with Gram-negative pneumonia in an intensive care unit population, *Am. Rev. Respir. Dis. 140*, 1585−1589.
2. Hoffken, G., and Niederman, M. S. (2002) Nosocomial pneumonia: The importance of a de-escalating strategy for antibiotic treatment of pneumonia in the ICU, *Chest 122*, 2183-2196.
3. Raymond, D. P., Pelletier, S. J., Evans, H. L., Pruett, T. L., and Sawyer, R. G. (2003) Impact of antibiotic-resistant Gram-negative bacilli infections on outcome of hospitalized patients, *Crit. Care Med. 31*, 1035−1041.
4. Bang, R. L., Gang, R. K., Sanyal, S. C., Mokaddas, E., and Ebrahim, M. K. (1998) Burn septicaemia: An analysis of 79 patients, *Burns 24*, 354−361.
5. Bang, R. L., Sharma, P. N., Sanyal, S. C., and Al Najjadah, I. (2002) Septicaemia after burn injury: A comparative study, *Burns 28*, 746−751.
6. Pruitt, B. A., Jr., McManus, A. T., Kim, S. H., and Goodwin, C. W. (1998) Burn wound infections: Current status, *World J. Surg. 22*, 135−145.
7. Maschmeyer, G., and Braveny, I. (2000) Review of the incidence and prognosis of *Pseudomonas aeruginosa* infections in cancer patients in the 1990s, *Eur. J. Clin. Microbiol. Infect. Dis. 19*, 915−925.
8. Tummler, B., Bosshammer, J., Breitenstein, S., Brockhausen, I., Gudwius, P., Herrmann, C., Heuer, T., Kubesch, P., Mekus, F., Romling, U., Schmidt, K. D., Spangenberg, C., and Walter, S. (1997) Infections with *Pseudomonas aeruginosa* in patients with cystic fibrosis, *Behring Inst. Mitt. 98*, 249−255.
9. Brennan, A. L., and Geddes, D. M. (2002) Cystic fibrosis, *Curr. Opin. Infect. Dis. 15*, 175−182.
10. Manfredi, R., Nanetti, A., Ferri, M., and Chiodo, F. (2000) *Pseudomonas spp*. complications in patients with HIV disease: An eight-year clinical and microbiological survey, *Eur. J. Epidemiol. 16*, 111−118.
11. Hancock, R. E. W., and Speert, D. P. (2000) Antibiotic resistance in *Pseudomonas aeruginosa*: Mechanisms and impact on treatment, *Drug Resist. Updates 3*, 247−255.
12. Normark, B. H., and Normark, S. (2002) Evolution and spread of antibiotic resistance, *J. Intern. Med. 252*, 91−106.
13. Hahn, H. P. (1997) The type-4 pilus is the major virulence-associated adhesin of *Pseudomonas aeruginosa*−a review, *Gene 192*, 99−108.
14. Strom, M. S., and Lory, S. (1993) Structure−function and biogenesis of the type IV pili, *Annu. Rev. Microbiol. 47*, 565−596.
15. Merz, A. J., and So, M. (2000) Interactions of pathogenic *Neisseriae* with epithelial cell membranes, *Annu. Rev. Cell Dev. Biol. 16*, 423−457.
16. Farinha, M. A., Conway, B. D., Glaiser, L. M., Ellert, N. W., Irvin, R. T., Sherburne, R., and Paranchych, W. (1994) Alteration of the pilin adhesin of *Pseudomonas aeruginosa* PAO results in normal pilus biogenesis but a loss of adherence to human pneumocyte cells and decreased virulence in mice, *Infect. Immun. 62*, 4118−4123.
17. Tang, H., Kays, M., and Price, A. (1995) Role of *Pseudomonas aeruginosa* pili in acute pulmonary infection, *Infect. Immun. 63*, 1278−1285.
18. Sheth, H. B., Glasier, L. M. G., Willert, N. W., Cachia, P., Kohn, W., Lee, K. K., Paranchych, W., Hodges, R. S., and Irvin, R. T. (1995) Development of an anti-adhesive vaccine for *Pseudomonas aeruginosa* targeting the C-terminal region of the pilin structural protein, *Biomed. Pept. Proteins Nucl. Acids 1*, 141−148.
19. Cachia, P. J. Glasier, L. M. G., Hodgins, R. R., Wong, W. Y., Irvin, R. T., and Hodges, R. S. (1998) The use of synthetic peptides

in the design of a consensus sequence vaccine for *Pseudomonas aeruginosa*, *J. Peptide Res. 52*, 289−299.
20. Cachia, P. J., and Hodges, R. S. (2003) Synthetic peptide vaccine and antibody therapeutic development: Prevention and treatment of *Pseudomonas aeruginosa*, *Biopolymers 71*, 141−168.
21. Irvin, R. T., Doig, P. C., Sastry, P. A., Heller, B., and Paranchych, W. (1990) Usefulness of equilibrium parameters of adhesion in predicting the outcome of competition for bacterial receptor sites on respiratory epithelial cells by *Pseudomonas aeruginosa* strains of heterologous pilus type, *Microb. Ecol. Health Dis. 3*, 39−47.
22. Irvin, R. T. (1993) Attachment and colonization of *Pseudomonas aeruginosa*: Role of the surface structures, in *Pseudomonas aeruginosa as an Opportunistic Pathogen* (Campa, M., Bendinelli, M., and Friedman, H., Eds.) pp 19−42, Plenum Press, New York.
23. Doig, P., Todd, T., Sastry, P. A., Lee, K. K., Hodges, R. S., Paranchych, W., and Irvin, R. T. (1988) Role of pili in adhesion of *Pseudomonas aeruginosa* to human respiratory epithelial cells, *Infect. Immun. 56*, 1641−1646.
24. Doig, P., Sastry, P. A., Hodges, R. S., Lee, K. K., Paranchych, W., and Irvin, R. T. (1990) Inhibition of pilus-mediated adhesion of *Pseudomonas aeruginosa* to human buccal epithelial cells by monoclonal antibodies direct against pili, *Infect. Immun. 58*, 124−130.
25. Irvin, R. T., Doig, P., Lee, K. K., Sastry, P. A., Paranchych, W., Todd, T., and Hodges, R. S. (1989) Characterization of the *Pseudomonas aeruginosa* pilus adhesin: Confirmation that the pilin structural protein subunit contains a human epithelial cell-binding domain, *Infect. Immun. 57*, 3720−3726.
26. Lee, K. K., Doig, P., Irvin, R. T., Paranchych, W., and Hodges, R. S. (1989) Mapping the surface regions of *Pseudomonas aeruginosa* PAK pilin: The importance of the C-terminal region for adherence to human buccal epithelial cells, *Mol. Microbiol. 11*, 1493−1499.
27. Lee, K. K., Sheth, H. B., Wong, W. Y., Sherburne, R., Paranchych, W., Hodges, R. S., Lingwood, C. A., Krivan, H., and Irvin, R. T. (1994) The binding of *Pseudomonas aeruginosa* pili to glycosphingolipids is a tip-associated event involving the C-terminal region of the structural pilin subunit, *Mol. Microbiol. 11*, 705−713.
28. Campbell, A. P., McInnes, C., Hodges, R. S., and Sykes, B. D. (1995) Comparison of NMR solution structures of the receptor binding domains of *Pseudomonas aeruginosa* pili strains PAO, KB7, and PAK: Implications for receptor binding and synthetic vaccine design, *Biochemistry 34*, 16255−16268.
29. Campbell, P. A., Wong, W. Y., Houston, M., Jr., Schweizer, F., Cachia, P. J., Irvin, R. T., Hindsgaul, O., Hodges, R. S., and Sykes, B. D. (1997) Interaction of the receptor binding domains of *Pseudomonas aeruginosa* pili strains PAK, PAO, KB7, and P1 to a cross-reactive antibody and receptor analog: Implications for synthetic vaccine design, *J. Mol. Biol. 267*, 382−402.
30. Merz, A. J., So, M., and Sheetz, M. P. (2000) Pilus retraction powers bacterial twitching motility, *Nature 407*, 98−102.
31. Mattick, J. S. (2002) Type IV pili and twitching motility, *Annu. Rev. Microbiol. 56*, 289−314.
32. O'Toole, G. A., and Kolter, R. (1998) Flagellar and twitching motility are necessary for *Pseudomonas aeruginosa* biofilm development, *Mol. Microbiol. 30*, 295−304.
33. Stoodley, P., Sauer, K., Davies, D. G., and Costerton, J. W. (2002) Biofilms as complex differentiated communities, *Annu. Rev. Microbiol. 56*, 187−209.
34. Klausen, M., Heydorn, A., Ragas, P., Lambertsen, L., Aaes-Jørgensen, A., Molin, S., and Tolker-Nielsen, T. (2003) Biofilm formation by *Pseudomonas aeruginosa* wild type, flagella, and type IV pili mutants, *Mol. Microbiol. 48*, 1511−1524.
35. Abraham, S. N., Jonsson, A. B., and Normark, S. (1998) Fimbriae-mediated host-pathogen cross-talk, *Curr. Opin. Microbiol. 1*, 75−81.
36. DiMango, E., Ratner, A. J., Tabibi, S., and Prince, A. (1998) Activation of NF-κB by adherent *Pseudomonas aeruginosa* in normal and cystic fibrosis respiratory epithelial cells, *J. Clin. Invest. 101*, 2598−2607.
37. Jendrossek, A., Fillon, A., Belka, C., Müller, I., Puttkammer, B., and Lang, F. (2003) Apoptotic response of Chang cells to infection with *Pseudomonas aeruginosa* strains PAK and PAO-I: Molecular ordering of the apoptosis signaling cascade and role of type IV pili, *Infect. Immun. 71*, 2665−2673.
38. Dubnau, D. (1999) DNA uptake in bacteria, *Annu. Rev. Microbiol. 53*, 217−244.
39. Bradley, D. E., and Pitt, T. L. (1974) Pilus dependence of four *Pseudomonas aeruginosa* bacteriophages with non-contractile tails, *J. Gen. Virol. 24*, 1−15.
40. Hazes, B., Sastry, P. A., Hayakawa, K., Read, R. J., and Irvin, R. T. (2000) Crystal structure of *Pseudomonas aeruginosa* PAK pilin suggests a main-chain-dominated mode of receptor binding, *J. Mol. Biol. 299*, 1005−1017.
41. Keizer, D. W., Slupsky, C. M., Kalisiak, M., Campbell, A. P., Crump, M. P., Sastry, P. A., Hazes, B., Irvin, R. T., and Sykes, B. D. (2001) Structure of a pilin monomer from *Pseudomonas aeruginosa*: Implications for the assembly of pili, *J. Biol. Chem. 276*, 24186−24193.
42. Yu, L., Lee K. K., Hodges, R. S., Paranchych, W., and Irvin, R. T. (1994) The pili of *Pseudomonas aeruginosa* strains PAK and PAO bind specifically to the carbohydrate sequence β-D-GalNAc-(1−4)β-D-Gal found in glycosphingolipids asialo-GM_1 and asialo-GM_2, *Infect. Immun. 62*, 5213−5219.
43. Sheth, H. B., Lee, K. K., Wong, W. Y., Srivastava, G., Hindsgaul, O., Hodges, R. S., Paranchych, W., and Irvin, R. T. (1994) The pili of *Pseudomonas aeruginosa* strains PAK and PAO bind specifically to the carbohydrate sequence βGalNAc(1−4)βGal in glycosphingolipids asialo-GM_1 and asialo-GM_2, *Mol. Microbiol. 11*, 715−723.
44. Parge, H. E., Forest, K. T., Hickey, M. J., Christensen, D. A., Getzoff, E. D., and Tainer, J. A. (1995) Structure of the fibre-forming protein pilin at 2.6 Å resolution, *Nature 378*, 32−38.
45. Craig, L., Taylor, R. K., Pique, M. E., Adair, B. D., Arvai, A. S., Singh, M., Lloyd, S. J., Shin, D. S., Getzoff, E. D., Yeager, M., Forest, K. T., and Tainer, J. A. (2003) Type IV pilin structure and assembly: X-ray and EM analyses of *Vibrio cholerae* toxin-coregulated pilus and *Pseudomonas aeruginosa* PAK pilin, *Mol. Cell 11*, 1139−1150.
46. Audette, G. F., Irvin, R. T., and Hazes, B. (2003) Purification, crystallization, and preliminary diffraction studies of the *Pseudomonas aeruginosa* strain K122-4 monomeric pilin, *Acta Crystallogr., Sect. D 59*, 1665−1667.
47. Leslie, A. G. W. (1992) Recent changes to the MOSFLM package for processing film and image plate data, *Joint CCP4/ESF-EAMCB Newsletter on Protein Crystallogr. 26*.
48. CCP4 (1994) The SERC (U.K.) collaborative computing project No. 4: A suite of programs for protein crystallography, *Acta Crystallogr., Sect. D 50*, 760−763.
49. Navaza, J. (1994) AMoRe: An automated package for molecular replacement, *Acta Crystallogr., Sect. A 50*, 157−163.
50. Lamzin, V. S., and Wilson, K. W. (1993) Automated refinement of protein models, *Acta Crystallogr., Sect. D 49*, 129−147.
51. Perrakis, A., Harkiolaki, M., Wilson, K. W., and Lamzin, V. S. (2001) *ARP/wARP* and molecular replacement, *Acta Crystallogr., Sect. D 57*, 1445−1450.
52. Read, R. J. (1997) Model phases: Probabilities and bias, *Methods Enzymol. 277*, 110−128.
53. McRee, D. E. (1999) XtalView/Xfit: A versatile program for manipulating atomic coordinates and electron density, *J. Struct. Biol. 125*, 156−165.
54. Pasloske, B. L., Sastry, P. A., Finlay, B. B., and Paranchych, W. (1988) Two unusual pilin sequences from different isolates of *Pseudomonas aeruginosa*, *J. Bacteriol. 170*, 3738−3741.
55. Murshudov, G. N., Vagin, A. A., and Dodson, E. J. (1997) Refinement of macromolecular structures by the maximum-likelihood method, *Acta Crystallogr., Sect. D 53*, 240−255.
56. Winn, M. D., Isupov, M. N., and Murshudov, G. N. (2001) Use of TLS parameters to model anisotropic displacements in macromolecular refinement, *Acta Crystallogr., Sect. D 57*, 122−133.
57. Brünger, A. T. (1992) Free *R* value: A novel statistical quantity for assessing the accuracy of crystal structures, *Nature 355*, 472−475.
58. Engh, R. A., and Huber, R. (1991) Accurate bond and angle parameters for X-ray protein-structure refinement, *Acta Crystallogr., Sect. A 47*, 392−400.
59. Sheldrick, G. M., and Schneider, T. M. (1997) SHELXL: High-resolution refinement, *Methods Enzymol. 277*, 319−343.
60. Laskowski, R. A., MacArthur, M. W., Moss, D. S., and Thornton, J. M. (1993) PROCHECK: A program to check the stereochemical quality of protein structures, *J. Appl. Cryst. 26*, 283−291.
61. Ramakrishnan, C., and Ramachandran, G. N. (1965) Stereochemical criteria for polypeptide and protein chain conformations II. Allowed conformations for a pair of peptide units, *Biophys. J. 5*, 909−933.

62. Craig, L., Pique, M. E., and Tainer, J. A. (2004) Type IV pilus structure and bacterial pathogenicity, *Nat. Rev. Microbiol. 2*, 363−378.
63. Marvin, D. A., Nadassy, K., Welsh, L. C., and Forest, K. T. (2003) Type-4 bacterial pili: Molecular models and their simulated diffraction patterns, *Fibre Diffraction Rev. 11*, 87−94.
64. Haas, R., Schwarz, H., and Meyer, T. F. (1987) Release of soluble pilin antigen coupled with gene conversion in *Neisseria gonorrhoeae*, *Proc. Natl. Acad. Sci. U.S.A. 84*, 9079−9083.
65. Kus, J. V., Tullis, E., Cvitkovitch, D. G., and Burrows, L. L. (2004) Significant differences in type IV pilin allele distribution among *Pseudomonas aeruginosa* isolates from cystic fibrosis (CF) versus non-CF patients, *Microbiology 150*, 1315−1326.
66. McInnes, C., Sonnichsen, F. D., Kay, C. M., Hodges, R. S., and Sykes, B. D. (1993) NMR solution structure and flexibility of a peptide antigen representing the receptor binding domain of *Pseudomonas aeruginosa*, *Biochemistry 31*, 13432−13440.
67. Campbell, A. P., Bautista, D. L., Tripet, B., Wong, W. Y., Irvin, R. T., Hodges, R. S., and Sykes, B. D. (1997) Solution secondary structure of a bacterially expressed peptide from the receptor binding domain of *Pseudomonas aeruginosa* pili strain PAK: A heteronuclear multidimensional NMR study, *Biochemistry 36*, 12791−12801.
68. Wong, W., Campbell, A. P., McInnes, C., Sykes, B. D., Paranchych, W., Irvin, R. T., and Hodges, R. S. (1995) Structure−function analysis of the adherence-binding domain on the pilin of *Pseudomonas aeruginosa* strains PAK and KB7, *Biochemistry 34*, 12963−12972.
69. Suh, J.-Y., Spyracopoulos, L., Keizer, D. W., Irvin, R. T., and Sykes, B. D. (2001) Backbone dynamics of receptor binding and antigenic regions of a *Pseudomonas aeruginosa* pilin monomer, *Biochemistry 40*, 3985−3995.
70. Kraulis, J. (1991) MOLSCRIPT: A program to produce both detailed and schematic plots of protein structures, *J. Appl. Crystallogr. 24*, 946−950.
71. Merritt, E. A., and Bacon, D. J. (1997) Raster3D photorealistic molecular graphics, *Methods Enzymol. 277*, 505−524.

BI048957S